DOI: 10.1002/ejic.201100007

The Relationship between the Electrochemical and Chemical Oxidation of Ferrocene-Containing Carbonyl-Phosphane-β-Diketonato-Rhodium(I) Complexes – Cytotoxicity of [Rh(FcCOCHCOPh)(CO)(PPh_3)]

Jeanet Conradie[a] and Jannie C. Swarts*[a]

Keywords: Rhodium / Carbonyl complexes / Sandwich complexes / Cytotoxicity / Cyclic voltammetry

Ferrocene-containing rhodium(I) complexes of the type [Rh(FcCOCHCOR)(CO)(PPh_3)] with R = Fc (ferrocenyl), **1**, Ph (phenyl), **2**, CH_3, **3**, and CF_3, **4**, have been studied by cyclic voltammetry (CV) and bulk electrolysis techniques in CH_3CN. Two isomers for complexes **2**–**4** were detected. Results are consistent with Rh^I being oxidised first in an electrochemically irreversible two-electron transfer process, followed by the electrochemical reversible oxidation of each ferrocenyl group in a one-electron transfer process at slightly larger potentials. Only the E_{pa}(Rh) CV peaks resolved into two separate waves, each one being associated with an isomer. Slow isomerisation kinetics allowed the detection of two isomers of **2**–**4**. E_{pa}(Rh) and other compound physical parameters relates to the second-order rate constant for the oxidative addition of CH_3I to complexes **1**–**4** in acetone. Rhodium(III) reduction of oxidised **1**, **2**, **3** and **4** was observed at large negative potentials, while for [Rh(FcCOCHCOCF$_3$)(CH_3)(I)(CO)(PPh_3)] (**9**) it was observed at –1.492 V vs. Fc/Fc^+. Complex **2** was slightly more cytotoxic than the free $FcCOCH_2COPh$ ligand but less cytotoxic than cisplatin.

Introduction

Dicarbonylrhodium(I) complexes were made famous by the use of $[Rh(CO)_2(I)_2]^-$ as catalyst in the Monsanto process of converting methanol to acetic acid.[1] The rate-determining step of this homogeneous catalytic process involves oxidative addition. During oxidative addition, the redox state of the catalytic metal centre changes from rhodium(I) to rhodium(III). The kinetics of CH_3I oxidative addition in complexes of the type [Rh(β-diketonato)(CO)(PPh_3)], where the β-diketonato either contains a metallocene group,[2,3] or not,[4] have been thoroughly studied. In contrast, no electrochemical properties relating to ferrocene-containing β-diketonato carbonyl phosphane rhodium complexes have to the best of our knowledge been published. This is surprising because the reactivity of the rhodium-based catalytic species is related to the ease of rhodium oxidation during the course of the oxidative addition reaction.

Ferrocenes in general are studied as donors in energy transfer processes,[5] because they enhance catalytic activity in many reactions,[3,6] as high-burning rate composite propellant catalyst,[7] as anticancer drugs[8] and as a strong electron-donating substituent to manipulate electron density on complexes.[9,10] They are often used in electron transfer processes[11] due to their high thermal stability, reversible redox behaviour, and their chemical modification possibilities.

Since the ferrocenyl group is a strongly electron-donating group, it accelerates oxidative addition substantially.[3] Quantification ofthe effects that ligands have on the rhodium(I) redox (oxidation) potential may assist in designing effective rhodium-based catalysts. Several physical properties of such ligands may be used to predict the oxidation potential of a rhodium(I) centre in a specific class of compounds, here [Rh(RCOCHCOR′)(CO)(PPh_3)] complexes with R = ferrocenyl, Fc. These especially include Gordy scale group electronegativities, χ_R, of ligand side groups and "observed" ligand pK'_a values. Published pK_a data for free β-diketones, which exist as keto and enol isomers in equilibrium,[12] are referred to as "apparent pK'_a values"[13] because in the experimentally obtained pK'_a values, no attempt was made to separate enol and keto tautomer pK_a values. Gordy scale group electronegativities, χ_R, of the R groups of β-diketones $R'COCH_2COR$, are empirical numbers that express the combined tendency of not only one atom, but a group of atoms, like R = CF_3 or ferrocenyl (Fc), to attract electrons (including those in a covalent bond) as a function of the number of valence electrons, *n*, and the covalent radius, *r* (in Å), of groups as discussed elsewhere.[14] It is empirically adjusted to be aligned with Pauling atomic electronegativities.

It has previously been shown that the pK'_a of the β-diketone $R'COCH_2COR$ is linearly dependent on the sum of the group electronegativities of R′ and R, ($\chi_{R'} + \chi_R$) by pK'_a = –3.484($\chi_{R'} + \chi_R$) + 24.6.[3] The formal reduction

[a] Department of Chemistry, University of the Free State, P. O. Box 339, Bloemfontein 9300, Republic of South Africa
Fax: +27-51-444-6384
E-mail: swartsjc@ufs.ac.za

Supporting information for this article is available on the WWW under http://dx.doi.org/10.1002/ejic.201100007,

potentials (in V vs. Fc/Fc^+ in CH_3CN) of a series of ferrocene containing β-diketones $FcCOCH_2COR$, also relates[9] linear to the group electronegativity, χ_R, of R by $E^{o\prime} = 0.114\chi_R - 0.025$. Moreover, the sum of the group electronegativities of R′ and R of the β-diketonato ligand $(R'COCHCOR)^-$ coordinated to $[Rh(R'COCHCOR)(CO)(PPh_3)]$ was shown to determine the second-order rate constant, k_2, of oxidative addition of CH_3I to these rhodium complexes by the equation $\ln k_2 = -3.14(\chi_{R'} + \chi_R) + 10.0$.[3]

In this communication we specifically report on the influence of Gordy scale group electronegativities of side groups of ferrocenyl-containing β-diketones on the oxidation potential of the rhodium centre in the complexes $[Rh(FcCOCHCOR)(CO)(PPh_3)]$ with R = Fc, Ph, CH_3 and CF_3. We generalise our results by relating χ_R, β-diketone pK'_a, E_{pa} of the rhodium(I) centre and rhodium complex ν_{CO} IR stretching frequencies to each other, and more importantly, to the rate of CH_3I oxidative addition to these complexes via k_2, the second-order rate constant of this reaction. The cytoxicity of $[Rh(FcCOCHCOPh)(CO)(PPh_3)]$ is also discussed.

Results and Discussion

The electrochemical behaviour of $[Rh(FcCOCHCOR)(CO)(PPh_3)]$ complexes with R = ferrocenyl = $(C_5H_5)Fe(C_5H_4)$ = Fc, **1**, phenyl = C_6H_5, **2**, CH_3, **3** and CF_3, **4**, was studied in acetonitrile containing 0.100 mol dm^{-3} tetra-*n*-butylammonium hexafluorophosphate $\{[N(nBu_4)][PF_6]\}$ utilizing a glassy carbon working electrode. Choice of this solvent ensured a two-electron oxidation process for the electrochemical oxidation of the rhodium(I) centre to ensure that it is comparable with the two-electron chemical oxidation of rhodium(I) during oxidative addition with CH_3I. Complexes **1**–**4** have three (for **1**) or two (in **2**, **3** and **4**) metal redox centres; the iron nucleus of the ferrocenyl group(s) and the square planar rhodium(I) centre, see Scheme 1.

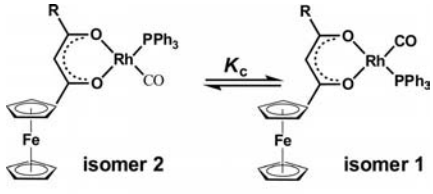

1 R = Fc, χ_{Fc} = 1.87
2 R = Ph, χ_{Ph} = 2.21, K_c = 0.56 (0.6)
3 R = CH_3, χ_{CH3} = 2.34, K_c = 0.23 (0.2)
4 R = CF_3, χ_{CF3} = 3.01, K_c = 0.68 (0.1-0.6)

Scheme 1. Rhodium complexes containing three (in **1**) or two (in **2**, **3** and **4**) metal redox centres. An equilibrium exists between the two isomers of $[Rh(FcCOCHCOR)(CO)(PPh_3)]$ giving K_c = [isomer 1]/[isomer 2][10] at 298 K in $CDCl_3$ (value in brackets is for CD_3CN) when R ≠ Fc. For **4**, K_c in CD_3CN gave poor resolved broad NMR peaks; from electrochemical studies, $K_c \approx 0.6$. The Rh^I nucleus of **1** is the most electron-rich in the series **1**–**4**, while for **4** it is the most electron deficient, see ref.[3]

Complex **1**, $[Rh(FcCOCHCOFc)(CO)(PPh_3)]$, contains a symmetrical β-diketonato ligand with two ferrocenyl side groups and exhibits three oxidation peaks during the cyclovoltammetric anodic cycle in the region 0–0.6 V vs. Fc/Fc^+, see Figure 1. The electrochemically irreversible anodic oxidation peak E_{pa} at 0.108 V vs. Fc/Fc^+ is assigned to the two-electron oxidation of rhodium(I) to rhodium(III). The two electrochemically reversible couples with formal reduction potentials, $E^{o\prime}$, of 0.200 and 0.312 V vs. Fc/Fc^+ correspond to the two successive one-electron redox process of each of the two ferrocenyl groups of the $(FcCOCHCOFc)^-$ ligand of $\mathbf{1}^{2+}$. The two ferrocenyl groups of the free ligand, $FcCOCH_2COFc$, are also oxidised in two successive redox steps during cyclic voltammetry.[9] The two ferrocene-based formal oxidation potentials of the free ligand are 89 and 92 mV smaller (less positive) than the corresponding $E^{o\prime}$ values of $\mathbf{1}^{2+}$.

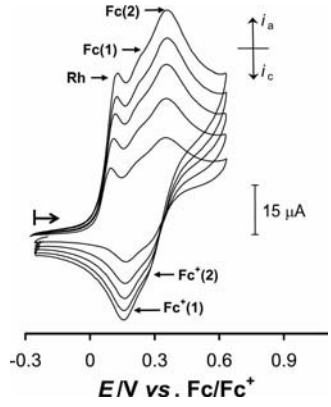

Figure 1. Cyclic voltammograms of a 1 mmol dm^{-3} solution of $[Rh(FcCOCHCOFc)(CO)(PPh_3)]$ (**1**), measured in 0.1 mol dm^{-3} $[N(nBu_4)][PF_6]/CH_3CN$ at scan rates of 50 (smallest currents), 100, 150, 200 and 250 mV s^{-1} on a glassy carbon working electrode at 25.0(1) °C. Scans are initiated in the positive direction, as indicated by the arrow. The rhodium and two ferrocene oxidation peaks are identified as Rh, Fc(1) and Fc(2), respectively.

Electron transfer approached electrochemical reversibility at slow scan rates with $\Delta E_p = E_{pa} - E_{pc}$ = 74 or 79 mV for the redox couples of the two ferrocenyl groups of **1** at scan rate 100 mV s^{-1}, see Table 1 (see Table S1 in the Supporting Information; scan rates 50–250 mV s^{-1}). Ideal electrochemical reversibility is characterised by ΔE_p = 59 mV.[15]

Different formal reduction potentials for side groups on symmetrical complexes in which mixed-valent (i.e. differently charged) intermediates are generated, here the ferrocenyl and the ferrocenium groups in $[Rh^{III}(Fc^+COCHCOFc)(CO)(PPh_3)]^{2+}$, are well known in systems that allow electron delocalisation, either through bridge mediated paths or from a direct metal–metal interaction.[16] The inequivalence of the ferrocenyl (Fc) and ferrocenium (Fc^+) groups of this intermediate is highlighted in terms of their group electronegativities: χ_{Fc} = 1.87, χ_{Fc+} = 2.82.[9,13,17] The electron-withdrawing power of the ferrocenium group is almost as high as that of the CF_3 group (χ_{CF3} = 3.01). As there is good communication (by conjuga-

Table 1. Electrochemical data for the ferrocenyl groups in [Rh(FcCOCHCOCR)(CO)(PPh_3)] and [Rh(FcCOCHCOCF_3)-(CH_3)(I)(CO)(PPh_3)] (**9**) from 0.7 mmol dm^{-3} solutions at a scan rate of 100 mV s^{-1} measured in 0.1 mol dm^{-3} [N(nBu$_4$)][PF_6]/CH_3CN on a glassy carbon electrode at 25.0(1) °C vs. Fc/Fc$^+$. Ferrocene itself showed under identical conditions reversible electrochemical behaviour (ΔE_p, = 66 mV, i_{pc}/i_{pa} = 1.00 at scan rate v = 100 mV s^{-1}, $E^{o\prime}$ = 0.077 V vs. a Ag/Ag$^+$ reference electrode).

	E_{pa} /V[a]	ΔE_p /mV[b]	$E^{o\prime}$ /V[c]	i_{pc} /μA[a]	i_{pc}/i_{pa}
1; R = Fc	0.237[d]	74[d]	0.200[d]	11[d],	1.00[d]
	(0.352)[e]	(79)[e]	(0.321)[e]	11[e]	(1.00)[e]
2; R = C_6H_5	0.331	117[g]	0.273	12	7.5 [f,g]
3; R = CH_3	0.301	102[g]	0.250	11	7.9 [f,g]
4; R = CF_3	0.441	122[g]	0.380	10	7.7 [f,g]
9	0.269	79	0.230	12.9	0.98

[a] Peak anodic potential or peak cathodic current. [b] $\Delta E_p = E_{pa} - E_{pc}$. [c] $E^{o\prime} = (E_{pa} + E_{pc})/2$. [d] Values for the first oxidized ferrocenyl group. [e] Values for the second oxidized ferrocenyl group. [f] Measured values for two unresolved ferrocenium reduction peaks. [g] ΔE_p and i_{pc}/i_{pa} are unusually large because of two unresolved Fc peaks from two isomers that lead to peak broadening.

tion) between the Fc and Fc$^+$ β-diketonato-pendent side groups on the pseudo-aromatic core of the intermediate [Rh^{III}(Fc$^+$COCHCOFc)(CO)(PPh_3)]$^{2+}$, oxidation of the second Fc group to yield the final oxidised species [Rh^{III}(Fc$^+$COCHCOFc$^+$)(CO)(PPh_3)]$^{2+}$ takes place at a more positive potential than observed for the oxidation of the first Fc group.

Scheme 2 represents the electrochemical processes associated with **1**.

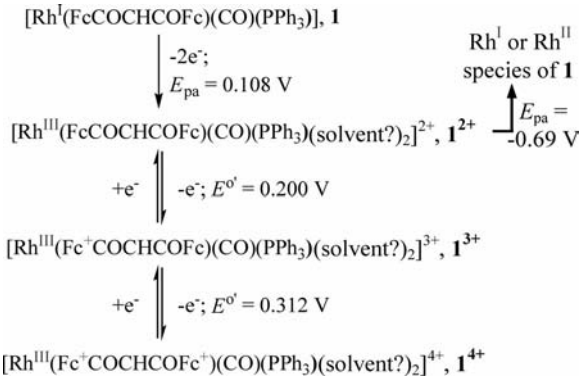

Scheme 2. Electrochemical scheme highlighting the electrochemical reversible ferrocene-based and electrochemical irreversible rhodium-based electron transfer processes. Species **1^{2+}** is a 14 electron complex that must be ligated by two additional ligands. The most likely candidate for this is the solvent, CH_3CN, but CO bridges and PF_6^- coordination are two further possibilities.

Complexes **2**–**4**, containing unsymmetrical β-diketonato ligands exist in solution as two isomers, see Scheme 1.[10] This equilibrium is slow to be reached, see the kinetic discussion below, and enabled us to observe each isomer by ^{1}H NMR separately, and to determine K_c values (defined in Scheme 1) in different solvents, including CD_3CN.[10] The CVs of **2**, **3** and **4** (Figure 2) are thus expected to exhibit two electrochemically irreversible anodic rhodium(I) oxidation peaks and two peaks that are associated with the ferrocenyl groups of the two isomers of **2**, **3** and **4**. These latter peaks could not be well resolved under our experimental conditions.

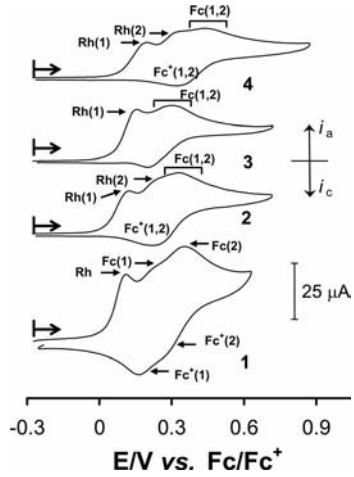

Figure 2. Cyclic voltammograms of 0.7 mmol dm^{-3} solutions of [Rh(FcCOCHCOR)(CO)(PPh_3)] complexes **1** (R = Fc), **2** (R = C_6H_5), **3** (R = CH_3) and **4** (R = CF_3) at scan rate 100 mV s^{-1} measured in 0.1 mol dm^{-3} [N(nBu$_4$)][PF_6]/CH_3CN on a glassy carbon working electrode at 25.0(1) °C. Complexes **2**, **3** and **4** exist as two isomers. The two rhodium and two unresolved ferrocene oxidation peaks of **2**, **3** and **4** are identified as Rh(1), Rh(2) and Fc(1,2). The Rh(2) peak of **3** overlaps indistinguishable with the ferrocenyl peaks. Complex **1** having a symmetrical β-diketonato ligand cannot have two isomers but it has two ferrocenyl groups, the redox peaks of which are labelled Fc(1) and Fc(2).

An alternative but less likely explanation for the multiple redox peaks observed in Figure 2 exists. Rather than assigning the two consecutively observed Rh$^I \rightarrow$ Rh^{III} oxidation peaks for **2**, **3** and **4** (Figure 2) to two isomeric forms as shown in Scheme 1, one may consider to assign the first oxidation Rh^I wave to a Rh$^I \rightarrow$ Rh^{II} conversion and the second to a Rh$^{II} \rightarrow$ Rh^{III} conversion as described for the five-coordinate complex [Rh^I(H)(CO)(PPh_3)$_3$].[18] We do not favour including identification of a rhodium(II) species in CH_3CN for the present compound series for the following reasons: Since four coordinate rhodium(II) complexes are known to be labile, except in the case where Rh^{II} dimers are coordinated to acetate ligands, we propose that, although the oxidation Rh$^I \rightarrow$ Rh^{III} in successive *observable* steps in CH_3CN as solvent is not impossible, it is rather unlikely. Experimentally if Rh$^I \rightarrow$ Rh^{II} oxidation corresponds to the first observed oxidation peak and Rh$^{II} \rightarrow$ Rh^{III} corresponds to the second, one would expect that the peak currents, i_{pa}, for Rh$^I \rightarrow$ Rh^{II} oxidation as well as for Rh$^{II} \rightarrow$ Rh^{III} oxidation should be the same for all complexes. This was not found to be the case. In addition, from the ferrocene waves, a one-electron transfer process in the present complexes under our experimental conditions is found to vary between 10 and 12 μA (Table 1). The values of the peak anodic currents for the first rhodium oxidation shown in Figure 2, i_{pa}(Rh1), of the first isomer of **2**, **3** and **4** measured 17, 21 and 15 μA, respectively (Table 2). This is too large for a one-electron transfer process. The sum of the two rhodium peak anodic currents, i_{pa}(Rh1) + i_{pa}(Rh2)

Table 2. Electrochemical and oxidative addition kinetic data related to rhodium(I) oxidation in [Rh(β-diketonato)(CO)(PPh_3)] complexes.

	β-diketonato	E_{pa}(Rh) /V [i_{pa} /μA][a]	E_{pc}(Rh) /V	pK'_a[b]	k_2 /mol^{-1} dm^3 s^{-1} [c]	ν_{CO} /cm^{-1} [d]
1	FcCOCHCOFc	0.108 [26][a]	–0.69	13.1(1)	0.155[h]	1977
2	$FcCOCHCOC_6H_5$	1: 0.123 [17], 2: 0.273 [8][a]	1: –0.75, 2: –[g]	10.41(2)	0.0409(3)	1977
3	$FcCOCHCOCH_3$	1: 0.154 [21], 2: 0.253 [3][a,e]	1: –0.86, 2: –0.45[g]	10.01(1)	0.0455(6)	1980
4	$FcCOCHCOCF_3$	1: 0.196 [15], 2: 0.327 [9][a]	1: –0.70, 2: –[g]	6.56(3)	0.00370(4)	1986
5	$C_6H_5COCHCOC_6H_5$	0.308[f]		9.35	0.00961	1979
6	$CH_3COCHCOC_6H_5$	0.336[f]		8.7	0.00930	1980
7	$CF_3COCHCOC_6H_5$	0.448[f]		6.3	0.00112	1983
8	$CF_3COCHCOCH_3$	0.491[f]		6.3	0.00146	1983
10	$CF_3COCHCOCF_3$	0.573[f]		4.71(1)		

[a] Oxidation peak potentials were measured on 0.7 mol dm^{-3} substrate concentration in 0.1 mol dm^{-3} [N(nBu$_4$)][PF_6]/CH_3CN on a glassy carbon electrode at 25.0(1) °C at a constant sweep rate of 100 mV s^{-1} referenced against Fc/Fc$^+$; values in square brackets are i_{pa} values for isomers 1 and 2, respectively. [b] pK'_a of the free β-diketone from ref.[13,20,21]. [c] Chemical oxidative addition rate constants k_2 are for the first step of the oxidative addition reaction between various [Rh{β-diketonato(CO)(PPh_3)}] complexes and CH_3I in acetone at 25.0(1) °C as described in ref.[2]. [d] The IR carbonyl stretching frequency of [Rh(β-diketonato)(CO)(PPh_3)] complexes, see ref.[10]. [e] Estimated values only because of closely overlapping peaks. [f] Results from ref.[22]. [g] E_{pc}(Rh) of the other isomer could not clearly be identified. [h] Value in chloroform.

for **2**, **3** and **4** was however 25, 24 and 24 μA, respectively, the expected values for two-electron transfer for the isomer mixture. In addition, a fast two-electron transfer process of a single compound having no isomers should exhibit a single i_{pa} peak of ca. 24 μA, i.e. twice the value of the ferrocene measurements. Complex **1** does not have any isomeric forms because the β-diketonato ligand is symmetrical. For this complex, only a single peak associated with Rh^I oxidation is observed, the size of which (i_{pa} = 26 μA) is also consistent with a two-electron transfer process, Figures 1 and 2, Table 2.

The large ferrocenyl ΔE_p values of **2**–**4** (Table 1) are not indicative of electrochemical irreversibility. Rather, it is the result of two unresolved ferrocenyl peaks from the two [Rh(FcCOCHCOR)(CO)(PPh_3)] isomers that lead to peak broadening. The difficulties that are encountered in resolving closely overlapping waves in cyclic voltammetry are well discussed elsewhere.[15,19]

To further strengthen the argument that the two sets of two-electron rhodium(I) oxidation peaks observed in Figure 2 corresponds to the two equilibrium species shown in Scheme 1, we attempted to follow the kinetics of conversion of isomer 2 to isomer 1 by ^{1}H NMR spectroscopy. Poor solubility and concomitant low integration accuracies of complexes **2**–**4** in CD_3CN prevented collection of reliable kinetic data to study the equilibrium isomerization kinetics of **2**–**4** in this solvent. For **2** and **3**, equilibrium in CD_3CN was reached in less than 5 min, and for **4**, equilibrium in CD_3CN was reached within one hour. However, in $CDCl_3$, it was possible to measure the conversion of isomer 2 to isomer 1 of complex **3** with time, see Figure 3. The half-life of this transformation is $t_{1/2}$ = 143 s and the observed rate constant of this transformation is k_{obs} = 0.0048(6) s^{-1} at 20 °C.

This slow rate of isomerization is very useful because it means in principle it is possible to distinguish between two different rhodium-based oxidation peaks during the electrochemical oxidation of the rhodium nucleuses of two isomers of [Rh(FcCOCHCOR)(CO)(PPh_3)]. The time required (less than 3 s at the slowest scan rate) in a CV experiment to

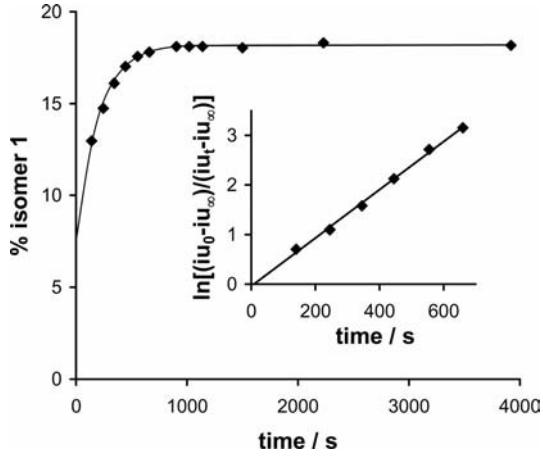

Figure 3. Time trace showing the conversion for isomer 2 to isomer 1 (reaction defined in Scheme 1) at 20 °C in $CDCl_3$ for [Rh(FcCOCHCOCH$_3$)(CO)(PPh_3)], **3**. Insert: A kinetic first order treatment of data for this process utilizing the first order kinetic equation $\ln(\frac{iu_0 - iu_\infty}{iu_t - iu_\infty}) = k_{obs}t$. iu_t is the average integration units of one H of isomer 1 in **3** at time t and is proportional to the concentration of isomer 1; iu_0 is the average integration unit at time t = 0 and iu_∞ the average integration units at time $t = \infty$ (i.e. after equilibrium has set in).

scan from peak potential Rh(1) which is associated with oxidation of the rhodium nucleus of the first isomer, to peak potential Rh(2), which is associated with the oxidation of the rhodium nucleus of the second isomer, is much shorter than $t_{1/2}$. This means rhodium oxidation in both isomers will take place on a CV timescale before concentration changes can be completed to reinstate K_c after the first rhodium isomer has been oxidised. Figure 4 shows the NMR of **3** in $CDCl_3$ at equilibrium as well as the NMR of **3** enriched in isomer 1.

The above described electrochemical results imply a two-electron transfer for the $Rh^{I/III}$ couple and a one-electron transfer process for the Fc/Fc$^+$ couple. This combined three-electron transfer process was confirmed by bulk electrolysis for **2**–**4**. Figure 5 shows current changes and the

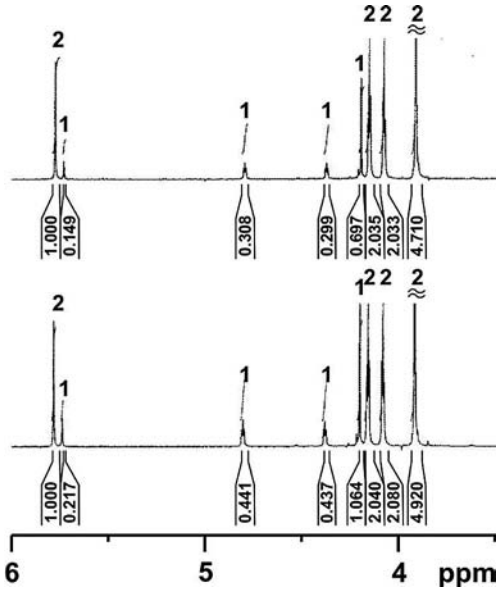

Figure 4. The 3–6 ppm region of a ^{1}H NMR spectrum of [Rh(FcCOCHCOCH$_3$)(CO)(PPh$_3$)], **3** enriched in isomer 1 (bottom) and in equilibrium with isomer 2 (top, isomers and K_c are defined in Scheme 1) at 293 K in $CDCl_3$ giving K_c = [0.217/1 + 0.441/2.040 + 0.437/2.080 + 1.064/4.920]/4 = 0.22[10] Isomer 1: 4.19 (s, 5 H, C_5H_5), 4.37 (t, 2 H, C_5H_4), 4.79 (t, 2 H, C_5H_4), 5.73 (s, 1 H, CH); Isomer 2: 3.91 (s, 5 H, C_5H_5), 4.08 (t, 2 H, C_5H_4), 4.15 (t, 2 H, C_5H_4), 5.78 (s, 1 H, CH).

amount of electrons transferred per molecule during the bulk electrolysis of **4** at an applied potential of 920 mV vs. Fc/Fc$^+$.

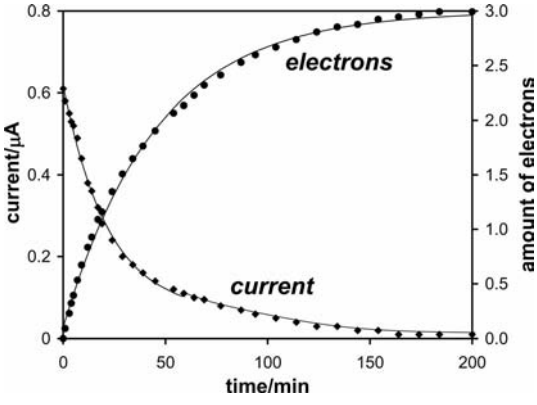

Figure 5. The electric current vs. time (i vs. t) response and total amount of electrons transferred per molecule ($\frac{It}{nF}$, n = number of mol of **4**, F = Faraday's constant) upon performing bulk electrolysis at 0.923 V vs. Fc/Fc$^+$ on [Rh(FcCOCHCOCF$_3$)(CO)(PPh$_3$)] (**4**).

Our observed two-electron transfer for rhodium(I) oxidation obtained in a 0.1 mol dm^{-3} [N(nBu$_4$)][PF$_6$]/CH$_3$CN solution is in agreement with those described by Lamprecht,[22] whom used the same solvent/electrolyte system as us to study **5**–**10** (see Table 2 for compound formulas), but contrasts the results obtained by Pombeiro[23] for other rhodium(I) complexes. Pombeiro[23] demonstrated a one-electron oxidation process for the oxidation of rhodium in [Rh(CH$_3$COCHCOCH$_3$)(CO)(PPh$_3$)], [Rh(CH$_3$COCHCOC$_6$H$_5$)(CO)(PPh$_3$)] (**6**) and [Rh(CF$_3$COCHCOC$_6$H$_5$)(CO)(PPh$_3$)] (**7**) in 0.2 mol dm^{-3} [N(nBu$_4$)][BF$_4$]/CH$_2$Cl$_2$ at a Pt-disc electrode. The big difference in the results of Pombeiro[23] and the present communication is the solvent used. Pombeiro used CH$_2$Cl$_2$, while in this study CH$_3$CN was preferred. Geiger,[24] and others[15a,25] have shown that the use of CH$_2$Cl$_2$ over CH$_3$CN and also [N(nBu)$_4$][B(C$_6$F$_5$)$_4$] over [N(nBu$_4$)][PF$_6$] as supporting electrolyte often lead to detection of unstable species such as ruthenocenium radical cations.

To establish whether it is possible to observe Rh^{III} reduction in our compounds, several experiments were performed. These are shown in Figure 6 for **3**. Upon scanning in a positive direction from –0.27 V till 0.71 V (bottom graph) the rhodium centre of both isomers of **3** were oxidized to a Rh^{III} species, the second of which was closely overlapping with the oxidation waves of the ferrocene centres (Table 2). During the reverse cycle, apart from observing the ferrocenium reduction at 0.199 V, two further small cathodic peaks were observed at –0.45 and –0.86 V respectively. These peaks are indicative of two separate Rh^{III} reductions associated with each of the two isomers of **3**. In a separate experiment, when the reversal potential of the first forward scan was lowered from 0.71 V to 0.185 V, the cathodic peak at –0.45 V was not observed (Figure 6, bottom grey scale). Since this reversal potential was small enough to disallow oxidation of the second Rh^{III} isomer during the first anodic sweep at ca. 0.253 V (Table 2) it can be concluded that the –0.45 V cathodic peak must belong to Rh^{III} reduction of one of the two isomers of oxidised **3** (isomer 2, Rh2 in our notation).

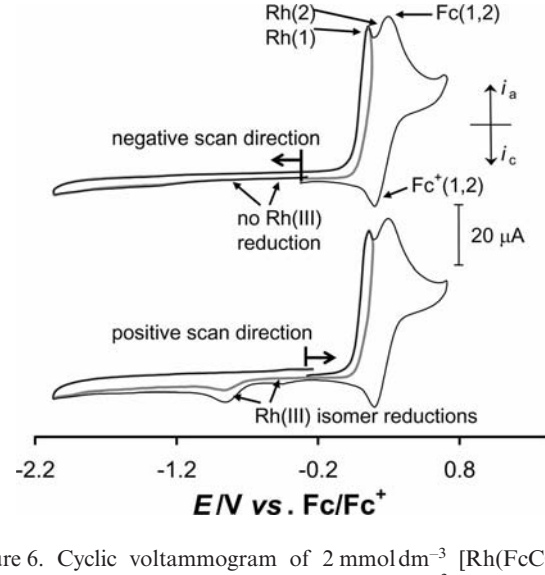

Figure 6. Cyclic voltammogram of 2 mmol dm^{-3} [Rh(FcCOCHCOCH$_3$)(CO)(PPh$_3$)] (**3**) measured in 0.1 mol dm^{-3} [N(nBu$_4$)][PF$_6$]/CH$_3$CN at a scan rate of 100 mV s^{-1} on a glassy carbon working electrode at 25.0(1) °C. The arrows indicate initial scan directions. See Table 1, footnote g, for explanation of small i_{pc}/i_{pa} ratios.

To show that the –0.86 V cathodic peak represents Rh^{III} reduction of the other oxidized isomer of **3** (Rh1 in our notation), another experiment was conducted in which the

scan direction was negative from the onset potential at –0.27 V, Figure 6 (top grey scale). Such a procedure meant no Rh^{III} generation has occurred before the scan direction was reversed. In this case, the –0.86 V cathodic peak was also absent which proved this peak was associated with Rh^{III} reduction of isomer 1 of oxidized **3** which is generated at E_{pa}(Rh1) = 0.154 V.

The electrochemical Scheme that summarizes the above described results for **2**, **3** and **4** are shown in Scheme 3.

The exact formula of the unstable in situ formed Rh^{III} complexes shown in Scheme 3 is unknown. Spectro-electrochemistry failed to give additional information on the potential structure. Rhodium(III) complexes normally are octahedral, so two further ligands is required to complete the newly generated rhodium(III) coordination sphere. The two ligands that will coordinate to these electrochemically in situ formed, Rh^{III} complex, apart from CO, PPh_3 and the β-diketonato, is unknown. However, it can only be species originating from the supporting electrolyte anions, PF_6^-, or more likely, solvent molecules, CH_3CN.

The structures of $[Rh^{I}(FcCOCHCOCF_3)(CO)(PPh_3)]$[26] and $[Rh^{III}(FcCOCHCOCF_3)(CH_3)(I)(CO)(PPh_3)]$ (**9**) was published[2] and the geometry of other Rh^{III}-β-diketonato derivatives were predicted by means of DFT geometry optimization techniques.[27] The electrochemistry of this known and stable Rh^{III} derivative **9** containing an un-oxidized ferrocenyl group were investigated cyclic voltammetrically to put the observed rhodium(III) reductions of complexes **1**–**4** in perspective (Figure 7). Complex **9** currently represents the only available stable rhodium(III) derivative of **1**–**4**, and its structure differs from that proposed in Scheme 3 by having the two solvent molecules replaced by an iodo and a methyl group. As was expected, no initial oxidation of Rh^{I} to Rh^{III} could be seen in the 0–0.5 V potential range, see Figure 7. Only a electrochemically reversible Fc/Fc^+ couple relating to the ferrocenyl group of [Rh(FcCOCH-

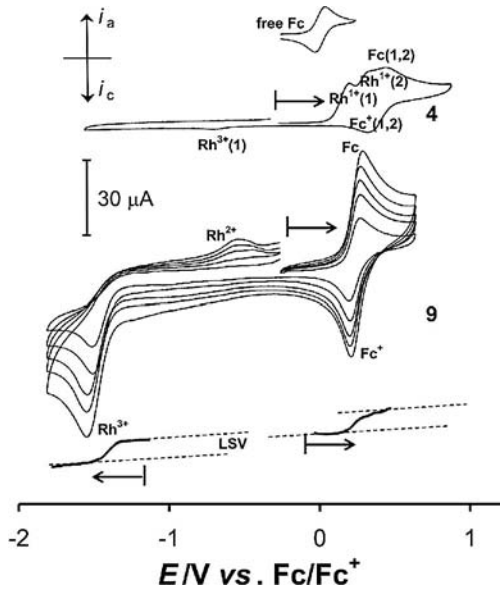

Figure 7. Cyclic voltammograms of 0.7 mmol dm^{-3} $[Rh^{I}(FcCOCHCOCF_3)(CO)(PPh_3)]$ (**4**) (top at 100 mV s^{-1}) and 1.5 mmol dm^{-3} $[Rh^{III}(FcCOCHCOCF_3)(CH_3)(I)(CO)(PPh_3)]$ (**9**) [middle at scan rates of 50, 100, 150, 200 and 250 (largest i_{pa}) mV s^{-1}] measured in 0.1 mol dm^{-3} $[N(nBu_4)][PF_6]/CH_3CN$ at a glassy carbon working electrode at 25.0(1) °C. The CV of **9** exhibits an electrochemically reversible Fc/Fc^+ couple which corresponds to the formal reduction potential of the ferrocenyl group of the $(FcCOCHCOCF_3)^-$ ligand coordinated to **9** and an electrochemically irreversible one-electron transfer process corresponding to the reduction of the rhodium(III) centre. The linear sweep voltammogram (LSV) of **9** (bottom) at a scan rate of 2 mV s^{-1} show a one-electron transfer process for both the oxidation of the ferrocenyl group and the reduction of rhodium of complex **9**.

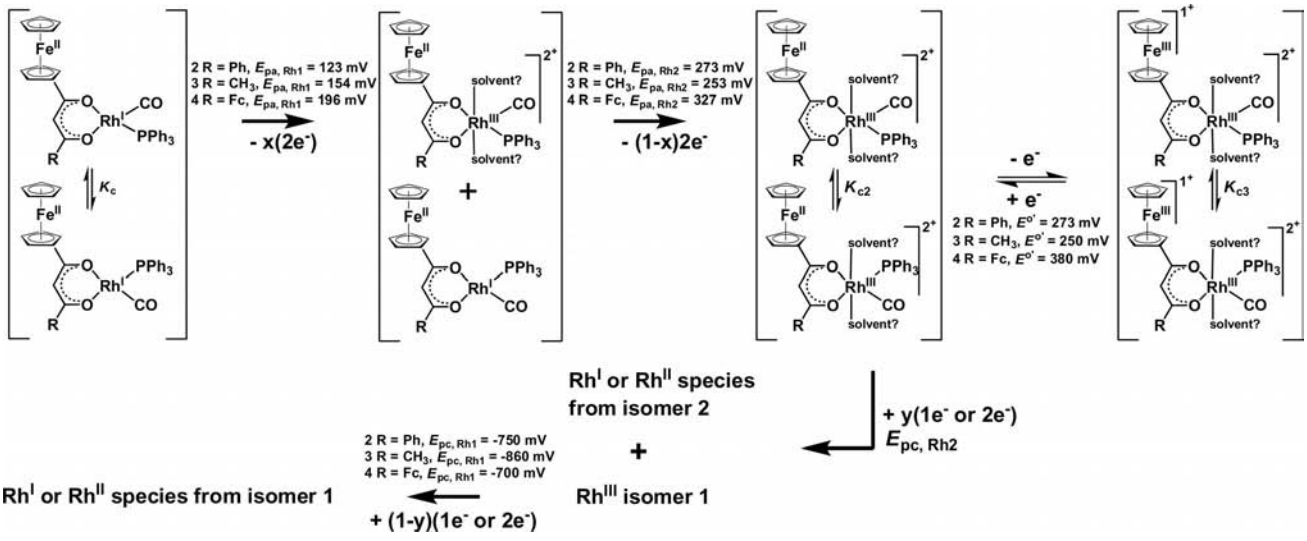

Scheme 3. Electrochemical oxidation of $[Rh(FcCOCHCOR)(CO)(PPh_3)]$ complexes **1**–**4**. Isomers in Scheme may interchange. *x* denotes the fraction of reduced rhodium(I) complexes existing as isomer that oxidizes first, while *y* denotes the fraction of oxidized compound existing as isomer 2 that is reduced on the reverse cycle. *x* and *y* are not necessarily the same. Rhodium(III) reduction is in the above scheme indicated to generate either rhodium(I) or rhodium(II) because it was not possible to determine the oxidation state of the reduced species unambiguously. However, the reduction product of **9**, $[Rh^{III}(FcCOCHCOCF_3)(CH_3)(I)(CO)(PPh_3)]$, was shown to be a rhodium(II) species (Figure 7).

Table 3. Electrochemical data for the oxidation and reduction of the ferrocenyl group and the rhodium nucleus of the complex $[Rh^{III}(FcCOCHCOCF_3)(CH_3)(I)(CO)(PPh_3)]$ (**9**) measured in 0.1 mol dm^{-3} $[N(nBu_4)][PF_6]/CH_3CN$ on a glassy carbon electrode at 25.0(1) °C vs. Fc/Fc^+. The concentration of the complex was 1.5 mmol dm^{-3} in CH_3CN.

	Ferrocenyl group					Rhodium nucleus			
v/mV s^{-1}	E_{pa}/V	ΔE_p/mV	$E^{o\prime}$/V	i_{pa}/μA	i_{pc}/i_{pa}	E_{pa}/V	E_{pc} /V	i_{pa}/μA	i_{pc}/μA
50	0.268	74	0.231	18.2	0.98	–	–1.536	23.3	–
100	0.269	79	0.230	25.8	0.98	–	–1.542	29.1	–
150	0.273	84	0.231	32.4	0.98	–0.459	–1.566	36.8	4.0
200	0.275	90	0.230	36.4	0.97	–0.504	–1.567	40.0	4.4
250	0.277	94	0.230	40.8	0.97	–0.517	–1.568	42.5	5.1

$COCF_3)(CH_3)(I)(CO)(PPh_3)]$ (**9**) with ΔE_p = 74 mV at scan rate 50 mV s^{-1} was observed in the potential range –0.2 till 1 V vs. Fc/Fc^+ (Table 3). The formal reduction potential of the ferrocenyl group in **9**, $E^{o\prime}$ = 0.230 V, is 150 mV less positive than the Fc/Fc^+ couple for $[Rh^{III}(FcCOCH-COCF_3)(CO)(PPh_3)(solvent?)_2]$. This implies the two unknown ligands of the in situ formed $[Rh^{III}(FcCOCH-COCF_3)(CO)(PPh_3)(solvent?)_2]$ complex must have strong electron withdrawing properties compared to CH_3 and I.

However, during the reverse cathodic cycle, reduction of the rhodium(III) centre of **9** was observed as at E_{pc} = –1.492 V vs. Fc/Fc^+ at a scan rate of 100 mV s^{-1}. This result parallel the rhodium(III) reduction of **4** also shown in Figure 7. The E_{pc} value of **4** is 0.75 V more positive than that of **9**, and like the potential of the ferrocenyl-based wave, is also consistent with the oxidised product of **4** having two stronger electron-withdrawing groups coordinated to it than methyl and iodo. The peak currents of the ferrocene oxidation and the rhodium(III) reduction are approximately the same (Table 3). This is consistent with a one-electron transfer process for each. Linear sweep voltammetry of **9** also shows a one-electron transfer process for both the oxidation of the ferrocenyl group and the reduction of rhodium of complex **9**. The reduced rhodium(II) species that formed at –1.492 V is re-oxidised at ca. –0.5 V in an electrochemically irreversible process.

The rhodium-based peak anodic potential of **1**–**4** is a measure of the energy required to remove electrons from the rhodium centre, i.e.

$$[Rh^{I}(\beta\text{-diketonato})(CO)(PPh_3)] + \text{energy} \rightarrow [Rh^{III}(\beta\text{-diketonato})(CO)(PPh_3)] + 2e^-$$

The more positive the rhodium centre becomes under the influence of the coordinating ligands, the more energy will be required to remove electrons from it. This corresponds to a higher E_{pa} (electrochemical oxidation) and slower kinetic rate of chemical (e.g. with CH_3I) oxidation. Parameters that are related to the electron density on the rhodium centre in $[Rh^{I}(\beta\text{-diketonato})(CO)(PPh_3)]$ is the pK'_a value of the β-diketone $R'COCH_2COR$ coordinated to the rhodium complex (R′ = Fc or any other group), and the group electronegativities $\chi_{R'}$ or χ_R of the R′ and R side groups on the β-diketonato ligand.[10] In turn, an increase in the electron density on the Rh metal centre will result in lower CO infrared stretching frequencies, ν_{CO}, in $[Rh^{I}(\beta\text{-diketonato})-(CO)(PPh_3)]$.[10]

With respect to group electronegativity sums, $(\chi_{R'} + \chi_R)$, and pK'_a values, the apparent acid strength of the free β-diketones $R'COCH_2COR$, it was shown in ref.[3] that

$$\ln k_2 = -3.14\,(\chi_{R'} + \chi_R) + 10.0 \quad (1a)$$

and that

$$\ln k_2 = 0.83\,pK'_a - 11.6 \quad (1b)$$

where k_2 is the second-order rate constant of the oxidative addition of CH_3I to **1**–**8** in acetone at 25.0(1) °C. From this study, the relationship between E_{pa}(Rh2) where Rh2 relates to the second isomer (see Scheme 1, Figure 2 and Table 2) and $\ln k_2$ for **1**–**8** is shown in Figure 8 (a), black line. The linear tendency between these data points fits the equation

$$\ln k_2 = -14.721\,E_{pa(Rh(2))} + 0.195;\ R^2 = 0.95 \quad (1c)$$

Similarly, the linear relationship between ferrocenyl $E^{o\prime}$ values summarize in Table 1 and k_2 (insert in Figure 8, a) was determined as

$$\ln k_2 = -20.5\,E^{o\prime}{}_{(Fc)} + 2.11;\ R^2 = 0.99 \quad (1d)$$

The plot of ν_{CO}, the carbonyl stretching frequencies of $[Rh(R'COCHCOR)(CO)(PPh_3)]$ vs. E_{pa}(Rh) was not as clearly linear as the E_{pa}(Rh2)/$\ln k_2$ relationship, Figure 8 (a, broken line). Especially complexes **2** and **4** were clearly off the predicted trend. By ignoring data for complexes **2** and **4**, the equation

$$\nu_{CO} = 16.1\,E_{pa(Rh)} + 1975;\ R^2 = 0.91 \quad (2a)$$

was fitted to the graph.

In ref.[10] it was shown that

$$\nu_{CO} = 5(\chi_{R'} + \chi_R) + 1959 \quad (2b)$$

and that

$$\nu_{CO} = -1.3\,pK'_a + 1993 \quad (2c)$$

By manipulation of Equations 1a and 2b, it can be shown that the activity of oxidative addition of CH_3I addition to $[Rh(R'COCHCOR)(CO)(PPh_3)]$ may be established as

$$\ln k_2 = -0.628\,\nu_{CO} + 1241$$

The linear trend between E_{pa} of Rh and the sum of the group electronegativities $\chi_{R'} + \chi_R$ in Figure 8 (b, broken line) indicates that the Rh^I core becomes increasingly diffi-

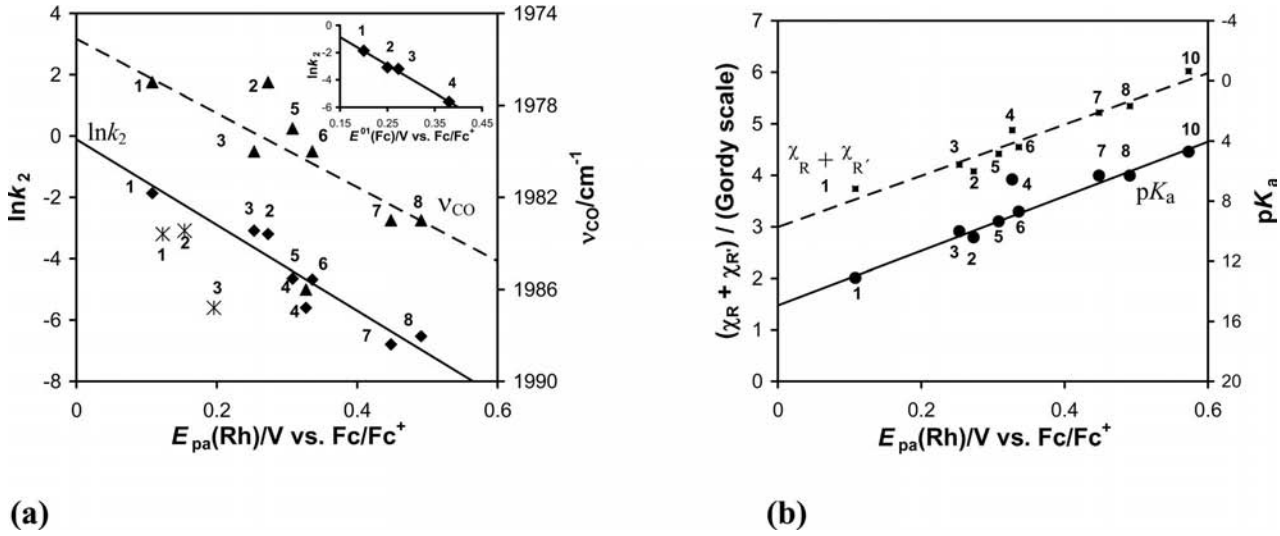

Figure 8. (a) Linear dependence (solid black line) between the kinetic parameter k_2 {the rate constant of the oxidative addition reaction between iodomethane and [Rh(β-diketonato)(CO)(PPh_3)]; k_2 was experimentally determined in ref.[3]} and E_{pa} of Rh in [Rh(β-diketonato)-(CO)(PPh_3)] measured at a scan rate of 100 mV s^{-1} and 25 °C. Points indicated with an asterisk * refer to the first Rh^I oxidation peak (Table 2) and were not used in the linear fits. The broken line represents the relationship between ν_{CO} and E_{pa} in the [Rh(β-diketonato)-(CO)(PPh_3)] complexes **1**–**8**. Insert: linear relationship between ferrocenyl formal reduction potentials and k_2. (b) The relationship between E_{pa}(Rh(2)) and the pK'_a of the free β-diketones (solid black line), or the sum of the group electronegativities of R′ and R ($\chi_{R'} + \chi_R$) of the β-diketonato ligand (R′COCHCOR)$^-$ coordinated to the metal complexes **1**–**9** (broken line).

cult to oxidize as the R groups of the coordinating β-diketonato ligands become more electronegative. More electron density is withdrawn from the rhodium(I) centre by the $(CF_3COCHCOCF_3)^-$ ligand of **10** than by any other β-diketonato ligand in the compound series **1**–**8** and **10**. Apparent group electronegativities in Gordy scale (in brackets) of the substituents R increase in the order Fc(1.87) < C_6H_5(2.21) ≈ CH_3(2.34) < CF_3(3.01),[9,13] which explains the progressive electron deficiency of the metal centre in moving from [Rh(FcCOCHCOFc)(CO)(PPh_3)] (**1**) to the [Rh(CF_3COCHCOCF_3)(CO)(PPh_3)] complex **10**. The E_{pa}(Rh)/($\chi_{R'} + \chi_R$) relationship of Figure 8 (b) fits the equation

$$(\chi_{R'}+\chi_R) = 5.02E_{pa(Rh)} + 2.95;\ R^2 = 0.96 \quad (3)$$

The linear relationship between the observed acidity of the free β-diketonato ligand, pK'_a and E_{pa}, Figure 8 (b), black solid line, were exceptionally good. Only **4** deviated slightly from the pK'_a – E_{pa} trend and was ignored in the data fitting that gave the equation

$$pK'_a = -18.2E_{pa}(Rh) + 14.9;\ R^2 = 0.99 \quad (4a)$$

From ref.[3], it was found that

$$pK'_a = -3.484(\chi_{R'} + \chi_R) + 24.6 \quad (4b)$$

Rearrangement of equation (2c) gives

$$pK'_a = -0.769\ \nu_{CO} + 1533 \quad (4c)$$

Combination and manipulation of the above equation sets resulted in equation array 5 as methods to estimate E_{pa}(Rh) for complexes of the type [Rh(β-diketonato)-(CO)(PPh_3)].

$$E_{pa(Rh)} = 0.191(\chi_{R'} + \chi_R) - 0.547;\ R^2 = 0.96 \quad (5a)$$

$$E_{pa(Rh)} = -0.054\ pK'_a + 0.817;\ R^2 = 0.99 \quad (5b)$$

$$E_{pa(Rh)} = 0.056\ \nu_{CO} - 111;\ R^2 = 0.91 \quad (5c)$$

$$E_{pa(Rh)} = -0.064\ \ln k_2 + 0.029;\ R^2 = 0.95 \quad (5d)$$

Equation array (6), obtained either by combination and manipulation of the equations given above, and confirmed by fitting the data of Tables 1 and 2 to a spread sheet fitting program, allows the estimation of $E^{o\prime}_{(Fc)}$ for [Rh(FcCOCHCOR)(CO)(PPh_3)]; χ_{Fc} = 1.87 in this equation array.

$$E^{o\prime}_{(Fc)} = 0.154(\chi_{R'} + \chi_R) - 0.377;\ R^2 = 0.96 \quad (6a)$$

$$E^{o\prime}_{(Fc)} = -0.028\ pK'_a + 0.552;\ R^2 = 0.95 \quad (6b)$$

$$E^{o\prime}_{(Fc)} = -0.049\ \ln k_2 + 0.107;\ R^2 = 0.99 \quad (6c)$$

$E^{o\prime}_{(Fc)}$ could not be estimated accurately from a fitted equation linking it to ν_{CO}, because the data correlation parameter R^2 (0.79) deviated to much from unity.

The cytotoxicity of ferrocene-containing complexes are frequently dependent on the formal oxidation potential of the ferrocenyl group. Related to ferrocene-containing alcohols, it was found that smaller $E^{o\prime}$ values lead to more favourable (higher) cytotoxicity.[28] In contrast, the free β-diketones $FcCOCH_2COR$ which were the ligands in **1**–**4** followed exactly the opposite trend.[8b] Two mechanisms by which the ferrocenyl group destroys antineoplastic growths were identified. The first was shown to involve homolytic action, i.e. radical induced electron transfer processes[29] between a ferrocenium group and water, inter alia to generate hydroxy radicals which cleave DNA strands. This implies a ferrocene-containing drug must, after it is administered to

the human body, first be oxidized by redox-active body enzymes to the ferrocenium species to show antineoplastic activity. Indications are that the cut-off formal reduction potential of the ferrocenyl group where this cannot happen any more is ca. +0.21 V vs. SCE (saturated calomel reference electrode) or 0.52 V vs. Fc/Fc^+.[8a,8b] $E^{o\prime}$ values of the ferrocenyl group of all four complexes **1**–**4** are less than 0.52 V, Table 1. In the second mechanism, the ferrocenyl group itself acts as a reducing agent when it reduces the tyrosyl radical of the R2 subunit of the enzyme ribonucleotide reductase.[30] The active site of dimeric R2 consists of a tyrosil radical and two Fe^{III} centers which are μ-oxo bridged. This enzyme catalyses the reduction of ribonucleotides to deoxyribonucleotides, a key step in DNA syntheses, and it's inactivation is therefore a goal in chemotherapy.[31] To investigate the possibility of compounds of the type [Rh(FcCOCHCOR)(CO)(PPh_3)] having antineoplastic properties, the cytotoxicity of **2** was determined against the HeLa cell line (human cervix epitheloid; ATCC CCL-2, American Type Culture Collection, Manassas, Virginia, USA). Cell survival was measured by means of the colorimetric 3-(4,5-dimethylthiazol-2-yl)-diphenyltetrazolium bromide (MTT) assay and a cell survival curve as a function of concentration of **2** is shown in Figure 9.

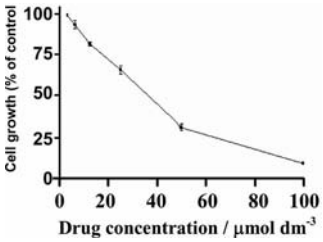

Figure 9. Effect of [Rh(FcCOCHCOPh)(CO)(PPh_3)], **2** on the survival of HeLa human cancer cells after 7 days of incubation measured as a percentage of untreated controls. Each end-point represents the mean of three experiments ± standard error of the mean.

The mean drug concentration of **2** from 3 experiments causing 50% cell growth inhibition, the IC_{50} value, was 42.2 μmol dm^{-3}. Complex **2** was substantially less cytotoxic than cisplatin [$Pt(NH_3)_3Cl_2$], which has IC_{50} = 2.3 μmol dm^{-3}, but slightly more cytotoxic than the free ligand, $FcCOCH_2COPh$, (IC_{50} = 54.2 μmol dm^{-3}) under identical conditions.[8b] The lowest IC_{50} value correspond to the more active compound. Compound **2** is about half as active against neoplastic cells as the cyclooctadiene complex [Rh(FcCOCHCOPh)(cod)] which exhibits IC_{50} = 28.3 μmol dm^{-3}.[32] These results are consistent with the betadiketonato ligand of **2** being responsible for most of the cell damage. The slightly higher activity of **2** as compared to the free ligand, $FcCOCH_2COPh$, must arise in part from the presence of the toxic CO group in **2**, but this is not the only reason. The rhodium centre itself also exhibits neoplastic activity as demonstrated for the cod complex.[32] Results are interpreted to imply that the (CO)(PPh_3) ligand combination of **2** is not as amenable to cell internalization as linear or cyclic aliphatics such as cod. Also, the Rh metal–CO ligand combination will probably cause **2** to be scavenged in vivo by the body's defense mechanism, the macrophage from the reticuloendothelial system, thereby limiting its capability to gain access to neoplastic growths in vivo.[33]

Conclusions

We showed in this study that in acetonitrile, complexes of the type [Rh(FcCOCHCOR)(CO)(PPh_3)] with R = Fc (**1**), Ph (**2**), CH_3 (**3**), or CF_3 (**4**) undergo irreversible two-electron electrochemical oxidation of the rhodium(I) centre before ferrocenyl oxidation takes place. Complexes **2**–**4** having unsymmetric β-diketonato ligands, i.e. R ≠ Fc, exist as two isomers in solution; both isomers exhibits distinct electrochemical behavior. Electrochemical observation of the rhodium and ferrocene oxidation of both isomers was possible because of the slow rate of isomerisation between isomers. Isomerisation of **3** was shown to have a half-life of 143 seconds in $CDCl_3$ at 20 °C utilizing ^1H NMR techniques.

An electrochemical study of the chemically prepared rhodium(III) complex [Rh^{III}(FcCOCHCOCF_3)(CH_3)(I)(CO)(PPh_3)] clearly showed a one-electron rhodium(III) reduction process at –1.492 V vs. Fc/Fc^+, while Rh^{III} reduction of electrochemically generated Rh^{III} complexes of **1**–**4** was observed at higher potentials. E_{pa}(Rh) of **1**–**4** is related to the rate of chemical oxidative addition of CH_3I to **1**–**4** by $E_{pa(Rh)} = -0.064 \ln k_2 + 0.026$. Both the reactivity of **1**–**4** towards oxidative addition and E_{pa}(Rh) was shown to depend linearly on the relative electron richness of the rhodium nucleus. This led to linear relationships between complex reactivity expressed as $\ln k_2$ and β-diketonato pK'_a values, complex ν_{CO} infrared stretching frequencies. The cytotoxic determination of **2** showed that [Rh(FcCOCHCOPh)(CO)(PPh_3)] is not significantly more active against neoplastic growths than the free $FcCOCH_2COPh$ ligand despite the presence of both CO and the rhodium centre.

Experimental Section

Materials and Cytoxicity Determination: Complexes **1**–**4**[10] and **9**[26] were synthesized as described earlier. Dry acetonitrile for electrochemical measurements was obtained by refluxing under nitrogen over calcium hydride, distillation onto alumina for storage, and redistilled just prior to use. The supporting electrolyte, electrochemical grade [N(nBu$_4$)][PF_6] from Fluka, was used as received. Cytotoxicity tests were performed as described before.[8b]

Electrochemical Measurements: Cyclic voltammetry measurements on ca. 0.7–1.0 mmol dm^{-3} solutions of **1**–**4** and **9** in dry acetonitrile containing 0.100 mol dm^{-3} tetra-*n*-butylammonium hexafluorophosphate {[N(nBu$_4$)][PF_6], Fluka, electrochemical grade} as supporting electrolyte were conducted under a blanket of purified argon at 25.0(1) °C utilizing a BAS model CV-27 voltammograph interfaced with a personal computer. A three-electrode cell, which utilized a Pt auxiliary electrode, a glassy carbon working electrode with surface area 7.07 mm^2 pre-treated by polishing on a Buehler microcloth first with 1 micron and then 1/4 micron diamond paste,

and a Ag/Ag^+ reference electrode was used. The reference electrode was constructed from a silver wire inserted into a solution of 0.0100 mol dm^{-3} $AgNO_3$ and 0.1 mol dm^{-3} $[N(nBu_4)][PF_6]$ in CH_3CN in a luggin capillary with a vycor tip.[9,34] Data, uncorrected for junction potentials, were collected with an Adalab-PC™ and Adapt™ data acquisition kit (Interactive Microwave, Inc.) with locally developed software, and analyzed with Hyperplot (JHM International, Inc.). Successive experiments under the same experimental conditions showed that all formal reduction and oxidation potentials were reproducible within 5 mV. All cited potentials are reported against the Fc/Fc^+ couple as suggested by IUPAC,[35] but were experimentally measured against Ag/Ag^+. The Fc/Fc^+ couple exhibited under our experimental conditions $E^{o\prime}$ = 0.077 V vs. Ag/Ag^+, i_{pc}/i_{pa} = 0.98 and ΔE_p = 74 mV. Bulk electrolyses were carried out utilising a BAS CV-27 voltammograph at 25.0(1) °C in 2.5 cm^3 acetonitrile. A three-electrode cell equipped with a Pt wire auxiliary electrode [isolated from the sample by means of a 0.1 mol dm^{-3} $(nBu)_4NPF_6/CH_3CN$ salt bridge], a glassy carbon working electrode (electro-active area ± 3 cm^2) and the Ag/Ag^+ reference electrode described above were employed. Current readings and the integrated current (Coulomb units) were recorded manually at different times, *t*, during the course of the experiments. Constructing of decay currents was required due to the overlap of the different oxidation and reduction peaks. Realistic peak anodic and cathodic currents of the cyclic voltammograms of complexes **1**–**4** were determined by constructing a decay current for each overlapping peak according to a method described in Figure S1 in the Supplementary Material.

Supporting Information (see footnote on the first page of this article): A diagram to explain how peak currents and potentials may be estimated for closely overlapping peaks, and a Table giving potentials at scan rates of 50–250 mV s^{-1}.

Acknowledgments

Financial assistance from the Central Research Fund of the University of the Free State is gratefully acknowledged.

[1] a) P. M. Maitlis, A. Haynes, G. J. Sunley, M. J. Howard, *J. Chem. Soc., Dalton Trans.* **1996**, 2187; b) L. Cavallo, M. Sola, *J. Am. Chem. Soc.* **2001**, *123*, 12294; c) A. Haynes, P. M. Maitlis, G. E. Morris, G. J. Sunley, H. Adams, P. W. Badger, C. M. Bowers, D. B. Cook, P. I. P. Elliot, T. Ghaffer, H. Green, T. R. Griffin, M. Payne, J. M. Pearson, M. J. Taylor, P. W. Vickers, R. J. Watt, *J. Am. Chem. Soc.* **2007**, *126*, 2847; d) J. Jones, *Platinum Met. Rev.* **2000**, *44*, 94.

[2] J. Conradie, G. J. Lamprecht, A. Roodt, J. C. Swarts, *Polyhedron* **2007**, *26*, 5075.

[3] J. Conradie, J. C. Swarts, *Organometallics* **2009**, *28*, 1018.

[4] a) J. A. Venter, J. G. Leipoldt, R. van Eldik, *Inorg. Chem.* **1991**, *30*, 2207; b) G. J. J. Steyn, A. Roodt, J. G. Leipoldt, *Inorg. Chem.* **1992**, *31*, 3477; c) M. M. Conradie, J. Conradie, *Inorg. Chim. Acta* **2008**, *361*, 2285; d) N. F. Stuurman, J. Conradie, *J. Organomet. Chem.* **2009**, *694*, 259.

[5] F. Spanig, C. Kolvacs, F. Hauke, K. Ohlubo, F. Fukuzumi, D. M. Guldi, A. Hirsch, *J. Am. Chem. Soc.* **2009**, *131*, 8180.

[6] a) A. Klapars, K. R. Clampos, C. Chen, R. P. Volante, *Org. Lett.* **2005**, *7*, 1185; b) Q. Shen, S. Shekhar, J. P. Stambuli, J. F. Hartwig, *Angew. Chem.* **2005**, *117*, 1395; *Angew. Chem. Int. Ed.* **2005**, *44*, 1371; c) V. Percec, L.-Y. Bae, D. H. Hill, *J. Org. Chem.* **1995**, *60*, 1060.

[7] P. J. Swarts, M. Immelman, G. J. Lamprecht, S. E. Greyling, J. C. Swarts, *S. Afr. J. Chem.* **1997**, *50*, 208.

[8] a) J. C. Swarts, D. M. Swarts, M. D. Maree, E. W. Neuse, C. La Madeleine, J. E. van Lier, *Anticancer Res.* **2001**, *21*, 2033; b) J. C. Swarts, T. G. Vosloo, S. J. Cronje, W. C. Du Plessis, C. E. J. Van Rensburg, E. Kreft, J. E. Van Lier, *Anticancer Res.* **2008**, *28*, 2781; c) B. Weber, A. Serafin, J. Michie, C. E. J. Van Rensburg, J. C. Swarts, L. Baum, *Anticancer Res.* **2004**, *24*, 763.

[9] W. C. Du Plessis, J. J. C. Erasmus, G. J. Lamprecht, J. Conradie, T. S. Cameron, M. A. S. Aquino, J. C. Swarts, *Can. J. Chem.* **1999**, *77*, 378.

[10] J. Conradie, G. J. Lamprecht, S. Otto, J. C. Swarts, *Inorg. Chim. Acta* **2002**, *328*, 191.

[11] a) A. Auger, J. C. Swarts, *Organometallics* **2007**, *26*, 102; b) W. L. Davis, R. F. Shago, E. H. G. Langner, J. C. Swarts, *Polyhedron* **2005**, *24*, 1611.

[12] For a discussion of the kinetics of keto-enol conversion of ferrocene β-diketones see: W. C. Du Plessis, W. L. Davis, S. J. Cronje, J. C. Swarts, *Inorg. Chim. Acta* **2001**, *314*, 97. A general treatment of β-diketone tautomers can be found in: R. C. Mehrotra, R. Bphra, D. P. Gaur, *Metal β-diketonates and Allied Derivates*, Academic Press, London, **1978**.

[13] W. C. Du Plessis, T. G. Vosloo, J. C. Swarts, *J. Chem. Soc., Dalton Trans.* **1998**, 2507.

[14] a) P. R. Wells, in *Progress in Physical Organic Chemistry*, John Wiley & Sons, New York, **1968**; vol. 6, p. 111–145; b) R. E. Kagarise, *J. Am. Chem. Soc.* **1955**, *77*, 1377.

[15] a) H. J. Gericke, N. I. Barnard, E. Erasmus, J. C. Swarts, M. J. Cook, M. A. S. Aquino, *Inorg. Chim. Acta* **2010**, *363*, 2222; b) D. H. Evans, K. M. O'Connell, R. A. Peterson, M. J. Kelly, *J. Chem. Educ.* **1983**, *60*, 290; c) P. T. Kissinger, W. R. Heineman, *J. Chem. Educ.* **1983**, *60*, 702; d) J. J. Van Benshoten, L. Y. Lewis, W. R. Heineman, *J. Chem. Educ.* **1983**, *60*, 772; e) G. A. Mobbott, *J. Chem. Educ.* **1983**, *60*, 697.

[16] a) C. Creutz, H. Taube, *J. Am. Chem. Soc.* **1969**, *91*, 3988; b) M. J. Cook, I. Chambrier, G. White, E. Fourie, J. C. Swarts, *Dalton Trans.* **2009**, 1136; c) N. Van Order, W. E. Geiger, T. E. Bitterwolf, A. L. Reingold, *J. Am. Chem. Soc.* **1987**, *109*, 5680; d) D. T. Pierce, W. E. Geiger, *Inorg. Chem.* **1994**, *33*, 373; e) A. Auger, A. J. Muller, J. C. Swarts, *Dalton Trans.* **2007**, 3623; f) W. E. Geiger, N. Van Order, D. T. Pierce, T. E. Bitterwolf, A. L. Reingold, N. D. Chasteen, *Organometallics* **1991**, *10*, 2403.

[17] J. Conradie, T. S. Cameron, M. A. S. Aquino, G. J. Lamprecht, J. C. Swarts, *Inorg. Chim. Acta* **2005**, *358*, 2530.

[18] a) D. Menglet, A. M. Bond, K. Coutinho, R. S. Dickson, G. G. Lazarev, S. A. Olsen, J. R. Pilbrow, *J. Am. Chem. Soc.* **1998**, *120*, 2086; b) F. Barriere, W. E. Geiger, *Organometallics* **2001**, *20*, 2133; c) I. Kovacik, H. Gevert, M. Schmittel, R. Söllner, *Inorg. Chim. Acta* **1998**, *276*, 435.

[19] D. E. Richardson, H. Taube, *Inorg. Chem.* **1981**, *20*, 1287.

[20] J. Stary, *The Solvent Extraction of Metal Chelates*, MacMillan, New York, **1964**, p. 196.

[21] M. Ellinger, H. Duschner, K. Starke, *J. Inorg. Nucl. Chem.* **1978**, *40*, 1063.

[22] D. Lamprecht, G. J. Lamprecht, *Inorg. Chim. Acta* **2000**, *309*, 72.

[23] M. Fatima, G. C. da Silva, A. M. Trzeciak, J. J. Ziolkowski, A. J. L. Pombeiro, *J. Organomet. Chem.* **2001**, *620*, 174.

[24] a) F. Barriere, R. U. Kirss, W. E. Geiger, *Organometallics* **2005**, *24*, 48, and references cited therein; b) S. Trupia, A. Nafady, W. E. Geiger, *Inorg. Chem.* **2003**, *42*, 5480; c) F. Barriere, N. Camire, W. E. Geiger, U. T. Mueller-Westerhoff, R. Sanders, *J. Am. Chem. Soc.* **2002**, *124*, 7262; d) F. Barriere, W. E. Geiger, *J. Am. Chem. Soc.* **2006**, *128*, 3980; e) A. Nafady, T. T. Chin, W. E. Geiger, *Organometallics* **2006**, *25*, 1654; f) D. S. Chong, J. Slote, W. E. Geiger, *J. Electroanal. Chem.* **2009**, *630*, 28.

[25] a) J. C. Swarts, A. Nafady, J. H. Roudebush, S. Trupia, W. E. Geiger, *Inorg. Chem.* **2009**, *48*, 2156; b) E. Fourie, J. C. Swarts, I. Chambrier, M. J. Cook, *Dalton Trans.* **2009**, 1145; c) K. C. Kemp, E. Fourie, J. Conradie, J. C. Swarts, *Organometallics* **2008**, *27*, 353; d) I. Chambrier, D. L. Hughes, J. C. Swarts, B. Isara, M. J. Cook, *Chem. Commun.* **2006**, 3504.

[26] G. J. Lamprecht, J. C. Swarts, J. Conradie, J. G. Leipoldt, *Acta Crystallogr., Sect. C* **1993**, *49*, 82.
[27] For DFT calculated structures of the products of oxidative addition of CH_3I to [Rh(ThCOCHCOR)(CO)(PPh_3)] and [Rh(FcCOCHCOCF_3)(CO)(PPh_3)], see ref.[4c] and M. M. Conradie, J. J. Conradie, *S. Afr. J. Chem.* **2008**, *61*, 102.
[28] R. F. Shago, J. C. Swarts, C. E. J. Van Rensburg, *Anticancer Res.* **2007**, *27*, 3431.
[29] D. Osella, M. Ferrali, P. Zanello, F. Laschi, M. Fontani, C. Nervi, G. Carvigiolio, *Inorg. Chim. Acta* **2000**, *306*, 42.
[30] A. Liu, D. N. Leese, J. C. Swarts, A. G. Sykes, *Inorg. Chim. Acta* **2002**, *337*, 83.
[31] a) J. C. Swarts, M. A. S. Aquino, K.-Y. Lam, A. G. Sykes, *Biochim. Biophys. Acta Protein Struct. Mol. Enzymol. Biochim. Biophys. Acta* **1995**, *1247*, 215; b) J. C. Swarts, A. G. Sykes, *Anti-Cancer Drug Des.* **1994**, *9*, 41; c) J.-Y. Han, J. C. Swarts, A. G. Sykes, *Inorg. Chem.* **1996**, *35*, 4629; d) S. Nyholm, L. Thelander, A. Gräslund, *Biochemistry* **1993**, *32*, 11569; e) E. Artin, J. Wang, G. J. S. Lohman, K. Yokoyama, G. Yu, R. G. Griffin, G. Bar, J. Stubbe, *Biochemistry* **2009**, *48*, 11622.
[32] J. Conradie, J. C. Swarts, *Dalton Trans.* **2011**, DOI: 10.1039/C1DT00013F.
[33] M. D. Maree, E. W. Neuse, E. Erasmus, J. C. Swarts, *Metal-Based Drugs* **2008**, xdoi:10.1155/2008/217573.
[34] A. Auger, J. C. Swarts, *Organometallics* **2007**, *26*, 102.
[35] G. Gritzner, J. Kuta, *Pure Appl. Chem.* **1984**, *56*, 461.

Received: January 4, 2011
Published Online: April 14, 2011

